The extent of variability in the stellar wind of the O 7.5 giant Xi Persei

Henrichs, H.F.; Kaper, L.; Nichols-Bohlin, J.S.

Publication date
1994

Published in
Astronomy & Astrophysics

Astron. Astrophys. 285, 565–572 (1994)

ASTRONOMY AND ASTROPHYSICS

The extent of variability in the stellar wind of the O 7.5 giant ξ Persei*

H.F. Henrichs[1], **L. Kaper**[1], **and J.S. Nichols**[2]

[1] Astronomical Institute "Anton Pannekoek", University of Amsterdam, and Center for High Energy Astrophysics, Kruislaan 403, NL-1098 SJ Amsterdam, Netherlands

[2] Science Programs, Computer Sciences Corporation, 10000-A Aerospace Rd., Lanham-Seabrook, MD 20706, USA

Received 26 August 1993 / Accepted 16 September 1993

Abstract. Using high-time-resolution ultraviolet spectroscopy, we present evidence that variability in the stellar wind of the O 7.5 III(n)((f)) star ξ Per takes place essentially over the whole velocity range over which the wind is observable in absorption: from ~ -100 km s^{-1} in the Si IV line up to -2750 km s^{-1} in N V and C IV, about 400 km s^{-1} beyond the terminal velocity of the stellar wind. The variations in the absorption part of the P Cygni profile include the discrete absorption components (DACs), which represent the strongest manifestations of the wind variability. In contrast, the emission part of the profile is steady. The blue steep edge in the saturated P Cygni lines varies in concert with the DACs. The changes in the subordinate N IV line at 1718 Å at low velocity (~ -250 to ~ -800 km s^{-1}) are found to vary in concert with the appearance of DACs in the Si IV lines. This implies that DACs are formed in a region relatively close to the surface. An evaluation of the statistical significance of variations in IUE spectra is presented.

Key words: stars: early type – stars: individual ξ Per – stars: mass loss – ultraviolet: stars

1. Introduction

Winds of O-type stars, as observed in P Cygni-type lines in ultraviolet spectra, are variable on time scales down to hours (e.g. Henrichs 1984; Prinja & Howarth 1986; Henrichs 1988). Understanding this variability is a challenge for the radiation-driven wind theory (Castor et al. 1975; Kudritzki 1988; Owocki 1991; and references therein). The spectral changes are often easily observed as variable discrete absorption components (DACs) in unsaturated P Cygni lines. Because of their characteristic shape DACs have been recognized in single snapshots for more than a decade. Howarth & Prinja (1989) reported DACs in more than 80% of 203 O stars. No convincing interpretation exists, however, for the origin and nature of the DACs, in spite of many proposed explanations. Unanswered questions included: (1) What makes a stellar wind develop DACs?, (2) Where in the flow are the DACs formed?, (3) Which physical parameters determine the timescale?, and (4) Is their appearance an intrinsic property of any radiatively driven flow?

The time evolution of DACs has been studied in detail with IUE for a number of selected O stars, in particular ξ Per O 7.5 III(n)((f)) (Prinja et al. 1987) and 68 Cyg O7.5III:n((f)) (Prinja & Howarth 1988). It was found that DACs first appear as broad absorption features at intermediate velocity (around -1000 km s^{-1}) in the blue absorption part of the unsaturated Si IV resonance lines. These broad features evolve within a few days into narrow absorption components at high velocity (exceeding -2000 km s^{-1}). The DACs reappear in cycles which are of the order of the rotational timescale of the star (Prinja 1988; Henrichs et al. 1988). The asymptotic velocity of the DACs is interpreted as the terminal velocity ($=v_\infty$) of the bulk flow of the wind (Howarth & Prinja 1986; Henrichs et al. 1988; Howarth & Prinja 1989; see also Groenewegen & Lamers 1989). This velocity coincides well with the highest velocity at which the saturated P Cygni profiles are still black ($=v_{\rm black}$), and on these grounds Prinja et al. (1990) have determined terminal velocities of more than 250 OB stars, which replaced earlier work in which the terminal velocity was derived from the steep edge of saturated P Cygni lines. Absorption in this steep edge beyond v_∞ is interpreted as a "turbulent" velocity, where the velocity dispersion is caused by shocks, superposed on the flow (Lucy 1983; Owocki et al. 1988).

Wind variability is also observed in this steep edge (e.g. Henrichs et al. 1988; Henrichs 1991; Prinja 1991). Some observations seem to indicate that the appearance of DACs and the position and shape of the blue edge are correlated (Prinja 1991), but a one to one correspondence for each star is difficult to establish. There is, however, no doubt that the variations

Send offprint requests to: H.F. Henrichs

* Based on observations by the International Ultraviolet Explorer, collected at NASA Goddard Space Flight Center and Villafranca Satellite Tracking Station of the European Space Agency

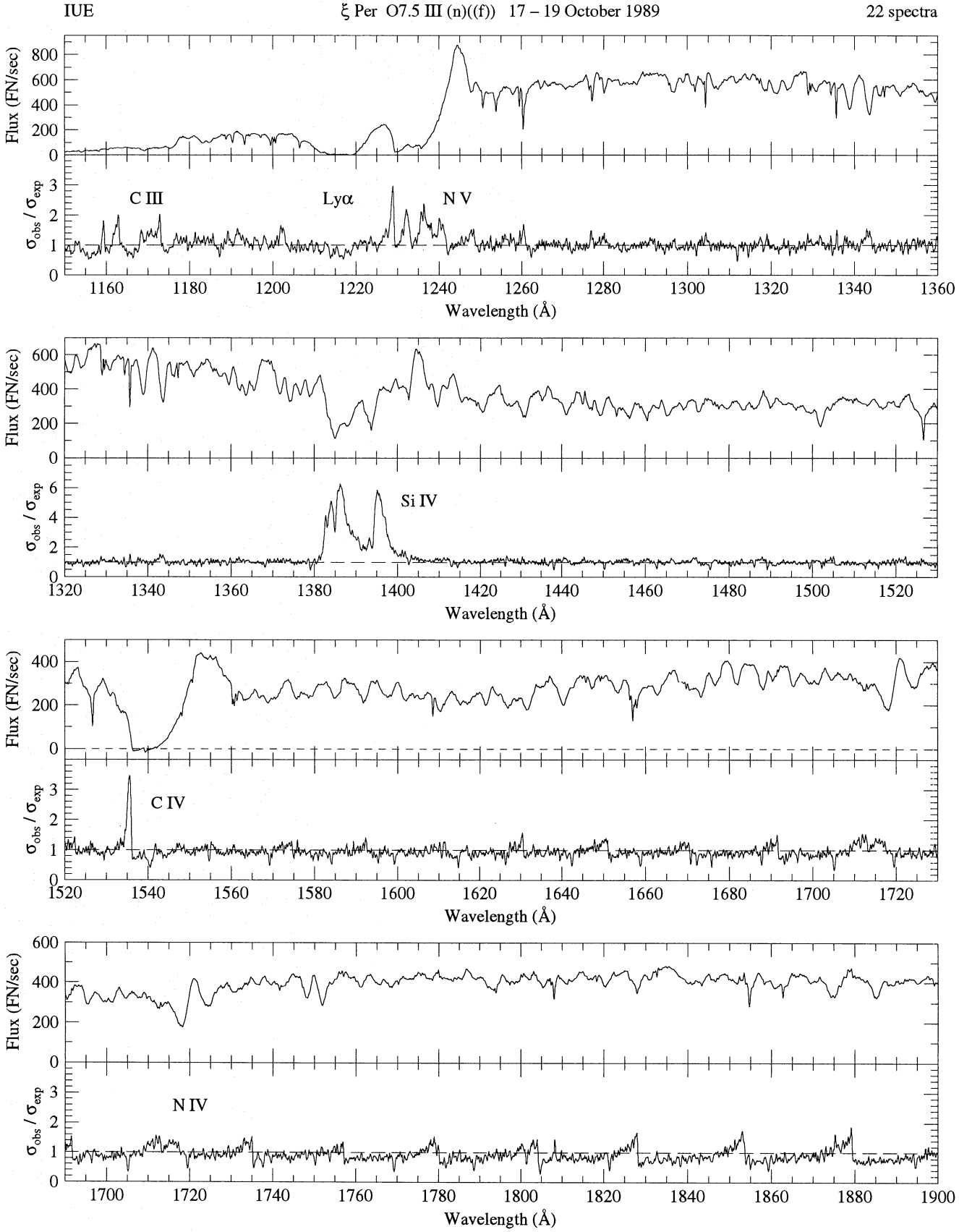

Fig. 1. Upper panels: average of 22 IUE spectra of ξ Per sampled at 0.1 Å. Lower panels: the corresponding σ-ratio, the amplitude of which characterizes the variability (see Sect. 3)

Table 1. Journal of IUE Observations of ξ Per, October 1989. The ground observatory is indicated in the last column (Goddard, with observers Nichols-Bohlin, Webb and Ewald, or VILSPA with observer Kaper)

#	Image SWP	Day October 1989	UT h:min:s	Mid Exp. HJD−2447810	
1	37328	17	5:37:18	6.735	G
2	37331		8:19:15	6.847	G
3	37334		11:05:06	6.963	G
4	37337		13:50:19	7.077	V
5	37340		15:55:28	7.164	V
6	37343		17:58:28	7.249	V
7	37346		20:10:15	7.341	V
8	37349		23:05:06	7.463	G
9	37352	18	1:29:48	7.563	G
10	37355		3:52:26	7.662	G
11	37358		6:20:58	7.765	G
12	37361		8:49:54	7.869	G
13	37364		11:19:20	7.972	G
14	37367		17:25:38	8.226	V
15	37370		19:43:39	8.322	V
16	37373		22:12:52	8.426	V
17	37376	19	0:33:44	8.524	G
18	37379		2:58:33	8.624	G
19	37382		5:28:33	8.728	G
20	37385		7:55:04	8.831	G
21	37388		10:50:14	8.952	G
22	37391		13:12:53	9.051	V
23	37393		17:35:41	9.233	V

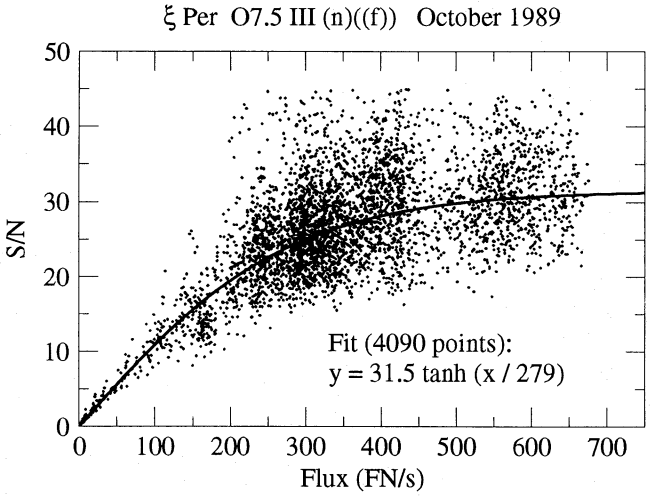

Fig. 2. Dots: Empirical signal-to-noise ratio determined from 22 spectra at 4090 different wavelengths. The curve is the best fit of a two-parameter function as indicated

occurring at velocities exceeding v_∞ are related to the propagation of DACs through the wind. Optical lines formed in the base of the stellar wind, such as He II at 4686 Å and Hα, often exhibit large variations. For several O stars it has been found that changes in these profiles occur on the same timescale as the variations in the stellar wind, and that these optical and UV variations are closely coupled in time (Henrichs 1991; Kaper et al. 1992).

In this paper we present 22 spectra of ξ Per obtained with the IUE satellite within 3 days in October 1989. The time resolution in this new sequence of spectra is better than in the timeseries analyzed by Prinja et al. (1987). We study the velocity range of the variability in several UV wind lines and how this variability is correlated in the different ions. Special attention is given to the low-velocity regime. An evaluation of the statistical significance of variability observed in IUE spectra is presented. The observational data and the reduction are described in the next section. How to characterize the significance level of variability is discussed in Sect. 3, followed by a description of the extent of variability in the wind of ξ Per. The time evolution of the variations is the subject of Sect. 5. We discuss the new results in the context of current stellar wind theory in Sect. 6. The last section summarizes our conclusions.

2. Observational data

In October 1989 a total of 23 spectra of the star ξ Per (HD 24912) were obtained within 3 days with the Short Wavelength Prime (SWP) camera in high dispersion on board the *International Ultraviolet Explorer* (IUE) satellite with an exposure time of 70 seconds in the large aperture. Table 1 gives the journal of observations. One image (SWP 32393) was strongly affected by unusually high background radiation and was discarded in this study in order to keep a homogeneous series. The geometrically and photometrically corrected spectra have been reduced in a standard manner with the STARLINK software package IUEDR (Giddings 1983a, 1983b). The background correction algorithm from Bianchi & Bohlin (1984) was included. Ripple corrections were applied following Barker (1984). Small corrections in the wavelength calibration were needed to obtain good alignment of the interstellar lines. Each spectrum was mapped onto an equidistant wavelength grid with spacing 0.1 Å. Gaps in the spectrum due to reseau marks were removed by linear interpolation through three points at either side of each gap. This procedure generates a very small amount of non-existent data, but this has no consequences for the results of the present paper. The average of the 22 spectra between 1150 and 1900 Å is displayed in Fig. 1. No attempt has been made to correct the fluxes for the wavelength-dependent sensitivity of the instrument. As no reliable correction procedure exists for the removal of the negative fluxes in the saturated part of the profile near the C IV 1550 line, we left these unchanged. Clearly distinguishable from the broad photospheric lines ($v \sin i = 200$ km s^{-1}, Conti & Ebbets 1977) is the fixed-pattern noise, which in principle could be removed with sophisticated methods. While all of these defects in the reduction of the spectra will increase slightly the errors involved in the determination of variability, these errors are negligible compared to the magnitude of the variations discussed here.

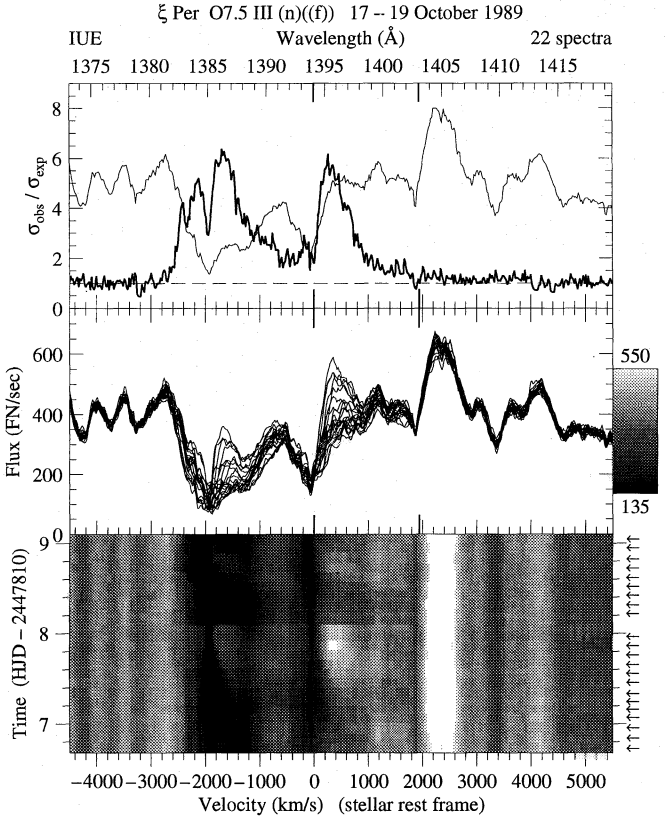

Fig. 3. Upper panel: temporal sigma spectrum, denoted by $\sigma_{obs}/\sigma_{exp}$ (thick line) of the region around the Si IV doublet superposed on the average spectrum (thin line) which was scaled down to fit on the graph. Thick elongated tick marks mark the rest wavelengths. Middle panel: overplot of all spectra. Lower panel: gray-scale presentation of the time sequence. The conversion scale from flux to gray level is attached to the middle panel. The velocity scale at the bottom is with respect to the blue component of the doublet and corrected for the radial velocity of the star. Arrows indicate mid-exposure times. The development of two discrete absorption components (DACs) can clearly be seen. Note also the edge variability (see Fig. 7 for a comparison with the C IV edge)

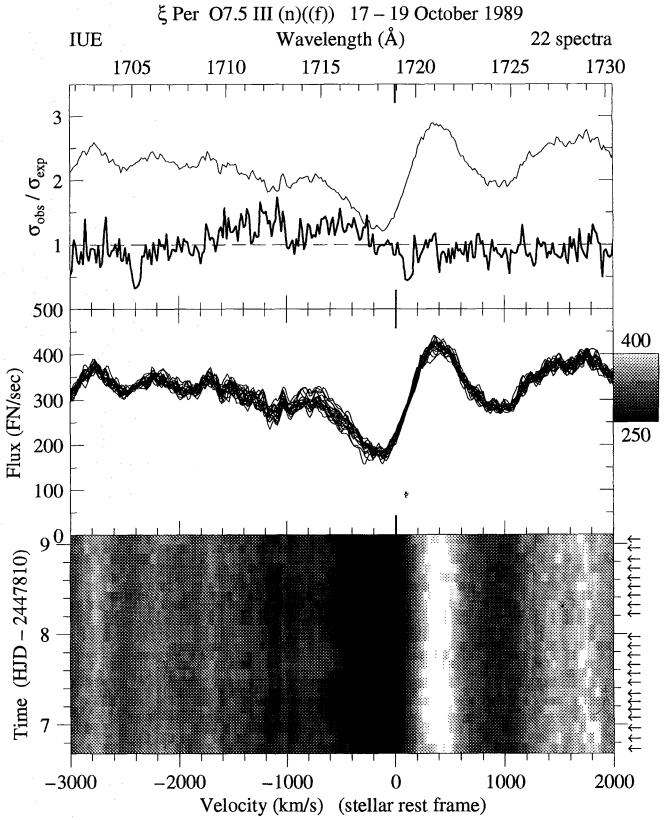

Fig. 4. Same as Fig. 3, but for the λ1718 subordinate line of N IV. The variations at low velocity occur concurrently to those in the DACs. The dips in the temporal sigma spectrum are caused by the removal of reseau marks

3. The significance level of variability

A simple overplot (see Figs. 3-6, middle panel) readily shows the well-known variable character of the UV resonance lines of ξ Per. To quantify the variability in IUE spectra in a statistically sound manner is, however, not trivial because of the rather complicated reduction procedure. To assign a significance level to the variability one needs an estimate for the expected noise at the wavelength considered. In IUE spectra, at each wavelength point the flux is a weighted average of the flux received at several pixels with each different exposure levels, whereas the sensitivity varies as a function of the pixel position on the camera. In addition, the order overlap regions and the fixed-pattern noise frustrate the determination of the pixel to pixel variations. The background determination is difficult at the low-wavelength end of the camera, because the spacing between the échelle orders becomes too small. Harris & Sonneborn (1987) give a detailed description of further specific properties of the camera used. The large wavelength region covered by the camera enables us, however, to study the instrumental plus photon noise level as a function of flux in an empirical way, using wavelength regions outside the variable resonance lines. We used the region between 1185 and 1800 Å, and also excluded the many small regions where échelle orders overlap, as in these intervals the noise level is higher because of the lower sensitivity at the edge of the orders.

We computed the average flux $F_{av}(\lambda)$ and the standard deviation $\sigma(\lambda)$ for each wavelength bin of 0.1 Å wide in the above mentioned "stable" regions over the sample of 22 spectra of ξ Per. In Fig. 2 the computed signal-to-noise ratio $S/N = F_{av}(\lambda)/\sigma(\lambda)$ is plotted as a function of $F_{av}(\lambda)$ for all 4090 points used. Although the scatter seems rather large, the two-parameter function

$$(S/N)_{av} = (31.5 \pm 0.2)\ \tanh\left(\frac{F}{278.8 \pm 4.5}\right), \qquad (1)$$

in which F is the flux, gives a satisfactory fit to the datapoints. We have assumed a Poisson distribution for the S/N values to calculate the errors, which gives a reduced $\chi^2 = 1.0$. The function described by Eq. (1) is drawn in Fig. 2. The asymptotic value of 31.5 represents the best S/N attainable in these spectra of ξ Per. We note that St. Louis et al. (1993) find a linear

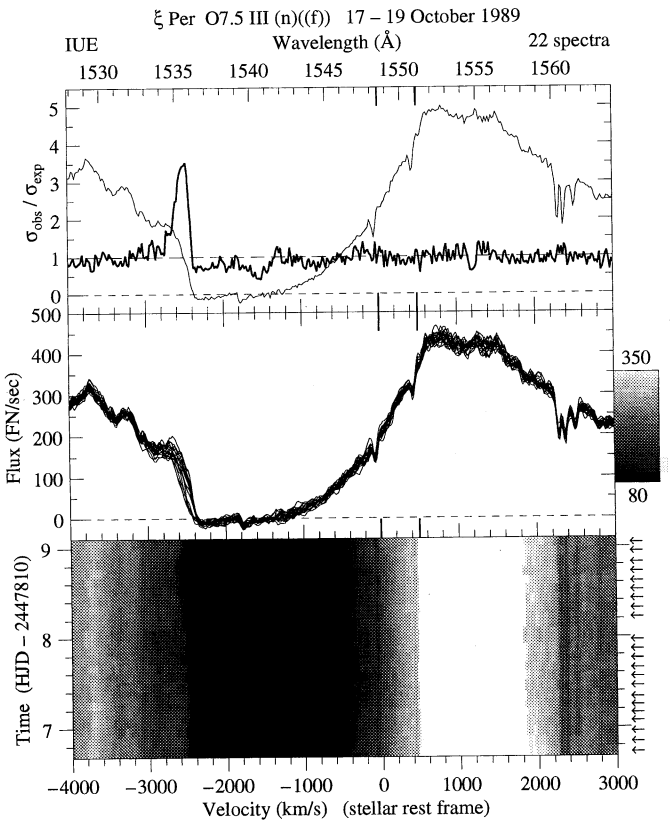

Fig. 5. Same as Fig. 3, but for the resonance doublet of C IV. The variability at the black outer edge is related to the DACs (see Fig. 7 for a comparison with the Si IV edge)

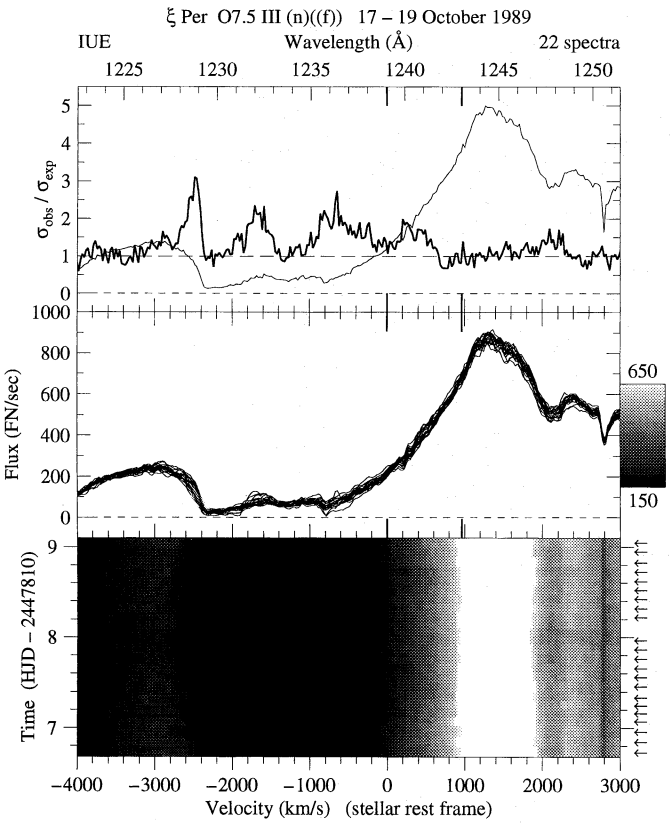

Fig. 6. Same as Fig. 3, but for the N V doublet. In spite of the lower quality of the data the characteristics appear the same as for C IV

relationship between the logarithm of the S/N and signal level (with a slope of 0.6) in their IUE spectra, which is very different from what we find in Fig. 2. Their function cannot represent the noise in our spectra, and a reason for this discordance might be that they used one typical spectrum to estimate the noise at different flux levels, whereas we use the average of all flux levels in 22 spectra. Our method eliminates some of the fixed pattern noise, implying the maximum S/N will be achieved at lower flux levels.

To characterize the variability, we follow the statistically rigorous method developed by Fullerton (1990). The significance of any variability is expressed in a temporal variance spectrum (TVS), which is in a good approximation

$$(\mathrm{TVS})_\lambda \approx \frac{1}{N-1}\sum_{i=1}^{N}\left[\frac{(F_i(\lambda)-F_{\mathrm{av}}(\lambda)}{\sigma_i(\lambda)}\right]^2, \qquad (2)$$

where N is the number of spectra and contributions from the instrumental and background noise are contained in $\sigma_i(\lambda)$. The TVS measures for each wavelength how the individually observed fluxes deviate from the expected flux. This analysis hinges on the knowledge of σ_i. Fullerton describes an elegant method to determine this quantity for each spectrum separately, depending on the used instrumentation and exposure level (and seeing conditions). As explained above, this is not a trivial matter for IUE spectra and we have chosen to simplify the evaluation of σ_i. We assume that all spectra are equally well exposed. This is justified in our case because of the very high degree of homogeneity of our sample due to stable spacecraft conditions. Furthermore, we assume that the analytical fit given in Eq. (1) represents the S/N for all spectra, and use this function to calculate σ_i. (We note that for a different set of spectra the numerical coefficients in Eq. (1) will be different.) In Figs. 1 and 3–6, we plot (after Fullerton) a temporal sigma spectrum TSS $\approx$ $(\mathrm{TVS})^{1/2}$, which can be considered as the ratio of the observed to the expected standard deviation $\sigma_{\mathrm{obs}}/\sigma_{\mathrm{exp}}$.

In this way we obtain a ratio equal to unity for points without significant variation, and a direct measure for the variability (in units of the expected noise level) for values greater than unity. From the lower panels in Fig. 1 one can easily determine the regions of interest for further study. The deficiencies in the smoothness of the obtained σ-ratio spectrum are readily attributed to the unavoidable simplifications in the adopted procedure. The regions of imperfect échelle order splicing are pronounced above 1600 Å. At these wavelengths the applied ripple correction as proposed by Barker (1984) is less applicable because the range of overlap decreases towards longer wavelengths. In some regions $\sigma_{\mathrm{obs}}/\sigma_{\mathrm{exp}} < 1$, e.g. in the saturated bottom of the C IV profile. This is a consequence of our overestimation of the noise at that low flux level, caused by the scarcity of calibration points in this flux range.

4. The extent of variability in stellar wind lines

The spectral lines of C III, N V, Si IV, C IV and N IV are variable (Fig. 1). The C III complex near 1175 Å is variable over the same range as the other ions (we confirmed the presence of the C III P Cygni profile in IUE spectra by consulting a spectrum of ξ Per obtained with the *Copernicus* satellite by Snow & Jenkins 1977), but a velocity range is difficult to give because the six C III lines overlap, so we exclude this line from further consideration. In Figs. 3 – 6 we compare the spectra of different ions, using the P Cygni lines of Si IV, N IV, C IV and N V, respectively. The velocity scale at the bottom axis has its zero point at the rest wavelength of the blue component of the doublet, corrected for the radial velocity of ξ Per (59 km s^{-1}, Gies & Bolton 1986). The rest wavelengths are indicated by a thick line. The upper panels give the ratio $\sigma_{obs}/\sigma_{exp}$, along with the average spectrum.

The largest amplitude of change occurs in the Si IV line (Fig. 3). The variability extends over both doublet components. The highest negative velocity at which significant variability can be found is $v_{max} = -2600$ km s^{-1}; the lowest velocity at which the wind appears to be variable is about $v_{min} \simeq -100$ km s^{-1} (red component). The latter is the lowest velocity where variation has been found. The maximum amplitude of the variations in the Si IV line is reached between ~ -1300 and ~ -2000 km s^{-1}. In the weak subordinate N IV line (Fig. 4) the variation as judged from the σ-ratio plot is weak, but significant, as can be seen from the variation in the grayscale plot. The two dips in the σ-ratio plot near 1705 and 1719 Å are caused by the removal of reseau marks. The σ-ratio is larger than unity between 1709 and 1713 Å, which is caused by the ripple transition, as can be seen from Fig. 1, and from comparison with spectra from different stars with approximate the same exposure level. The variation between -250 and -800 km s^{-1} is real. In the saturated C IV line we observe spectral variation only in the blue edge between $v_{max} \simeq -2750$ km s^{-1} and $v_{min} \simeq -2400$ km s^{-1} (Fig. 5). The dips near 1540 and 1555 Å are also due to reseau marks. The high-velocity end of the black bottom is at $v_{black} = -2350$ km s^{-1}. The N V resonance lines show similar blue-edge variability (Fig. 6), but the P Cygni profile also varies at low velocities, i.e. between ~ -400 (red doublet component) and ~ -1000 km s^{-1} (blue component). The measured quantities of the different lines are summarized in Table 2. It is remarkable that the emission parts of all profiles hardly show any variability. We conclude that the stellar wind of ξ Per is variable over a velocity range from -100 to at least -2750 km s^{-1}. In a previous paper (Prinja et al. 1987) a much smaller range was found.

Table 2. Variability in stellar wind lines of ξ Per. The table lists the minimum and maximum velocities at which significant variation is found. For the saturated lines the highest negative velocity of the black bottom of the profile is added. A typical uncertainty in the quoted values is less than 50 km s^{-1}

ion	λ (Å)	v_{min} (km s^{-1})	v_{black} (km s^{-1})	v_{max} (km s^{-1})
N IV	1718	-250		-800
Si IV	1402	-100		-2600
C IV	1548	-2400	-2350	-2750
N V	1242	-400	-2300	-2700

5. Time sequences and discrete absorption components

In the bottom panels in Figs. 3 – 6 the flux values of the 22 spectra have been converted into gray values according to the scale which is attached to the middle panel. The extreme flux values for the gray levels are chosen to optimize the contrast for the region of interest. For each spectrum a widening was applied in the spatial direction equal to half the time spacing to each of the neighboring mid-exposure time epochs. The mid-exposure times are indicated by arrows. The spectra are finally stacked in time order from bottom to top. In Fig. 3 the discrete absorption components (DACs) in the Si IV profile are easily recognized. DACs in an earlier epoch of ξ Per are well described in a previous extensive study (Prinja et al. 1987). In our sample, two DAC events are readily identified. Initially they are broad and can be distinguished from the underlying P Cygni profile around -1200 km s^{-1} at MJD = 7.2 and 8.3. In the course of half a day the center of the DACs migrate to about -2000 km s^{-1} and they become much narrower. In this stage they are easily recognized in individual spectra from which the common name *narrow* absorption components originates (e.g. Snow 1977). This qualifier has been replaced by *discrete*, in order to cover the whole phenomenon, rather than to restrict the name to a specific phase.

The subordinate N IV line at 1718 Å (Fig. 4) also shows significant variability, not recognized in our earlier study. This line shows a weak P Cygni type profile with the minimum flux at -250 km s^{-1}. No DACs can be identified, but the repeating behavior in N IV is very similar to the Si IV variability, except that most changes occur between -250 and -800 km s^{-1}. Because the N IV line is only formed in a relatively dense region, we consider the similarity in the behavior of these two ions as clear evidence that DACs develop from variable structures rather close to the star at rather low velocity, at any rate much lower than previously adopted and concluded from the Si IV behavior alone. (See the discussion below for additional evidence that the variability originates at low velocity.) The time behavior of the black C IV and N V edge is also correlated to the DACs in Si IV. This is illustrated in Fig. 7, which shows the remarkable parallel behavior near the Si IV and C IV edge. This strongly suggests that it is the much higher optical depth in the C IV line which prevents the detection of DACs in this line, and that the blue-edge variability is an extension of the DAC variability. This similar behavior was found by Henrichs et al. (1988) and Prinja (1991) for other O stars as well.

6. Discussion

We discuss several implications of the findings above with special emphasis on modeling the variability. DACs are undoubtedly formed in absorbing layers in the line of sight, projected against the stellar disk. The chance of finding DACs is not found to be a strong function of $v \sin i$, thus similar density structures

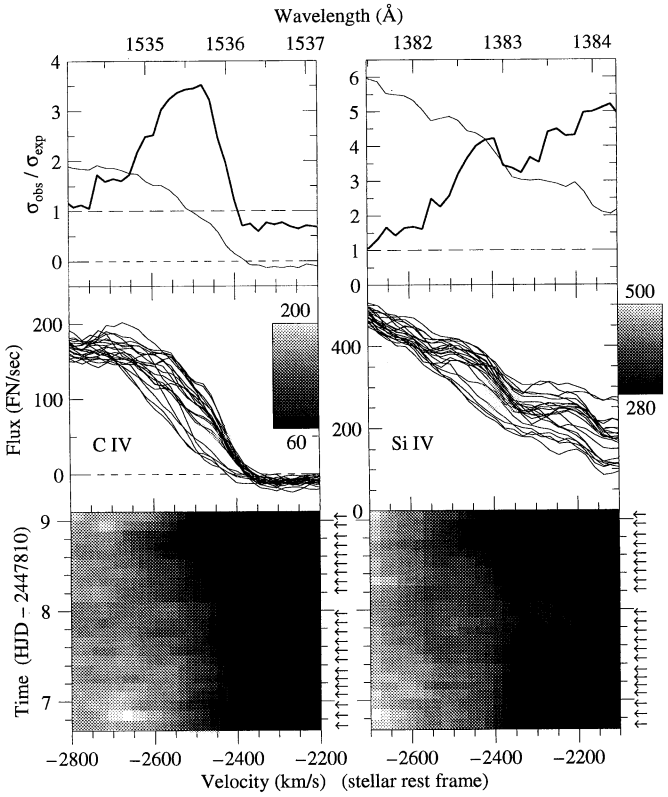

Fig. 7. A comparison of the edge variability in the C IV and Si IV lines. The parallel behavior strongly suggests that the regions where these lines are formed are the same, and that the variability in the DACs in Si IV actually extends to the blue-edge

must also be present in the emitting volume around the star. Since the emission part of the P Cygni profile does not vary substantially, the relative volume these structures occupy must be small and an upper limit for the integrated effect could be calculated for a given model. This will be complicated, however, if the wind is not spherically symmetric. The observed absorption in the DACs and the upper limit on the variability in the emission therefore pose limits on the lateral scale of the structures.

One of the explanations for the presence of DACs is that they originate in expanding high-density regions just behind shock fronts which develop from amplified radiative instabilities in the wind. The initially small-scale instabilities are in turn triggered by periodic perturbations from the surface of the star (Owocki et al. 1988; Owocki 1991). Puls et al. (1993) give, for the first time, a full calculation of a timeseries of calculated singlet P Cygni line profiles, with remarkable detail. Some, but not all, of the features of this 1-D hydrodynamical model calculations are similar to what is observed. The main difference is that stellar rotation was not yet incorporated by Puls et al., whereas the recurrence timescale seems to be correlated with the rotation period of the star (see also below). In any case, these calculations are very promising for unraveling the structure of early-type star winds.

Since DACs are not found at velocities below typically -1000 km s^{-1} one could argue against an interpretation in terms of instabilities starting from the stellar surface. The present paper shows that the variability occurs simultaneously in the DACs in Si IV and in the low velocity part of the N IV profile, at least in ξ Per. This demonstrates that variability in stellar wind lines is not restricted to DACs at intermediate velocities in unsaturated lines and blue-edge variations in saturated profiles, and that therefore the DACs have to be considered as the strongest manifestation of wind variability in general. This could support the radiative instability model, but a detailed comparison with calculated line profiles is needed to show if the variability at these low velocities are predicted. From Fig. 17 of Puls et al. (1993), which is calculated for slightly different stellar parameters than would be adopted for ξ Per, this low-velocity variability is present, but their calculation does apply more to our observed Si IV profile than to the N IV line, because the ion density of the latter decreases very rapidly outward. It should be emphasized that in the calculations by Owocki et al. (1991) and Puls et al. (1993) radiative instabilities develop from a further unspecified perturbation at or near the stellar surface. The growing instabilities may lead to the variability as observed in one DAC episode, but since the origin of the perturbation is not specified, it still remains unclear why new DACs should develop. A typical recurrence timescale for DACs is on the order of days, likely related to the stellar rotation period (Henrichs et al. 1988; Prinja 1988). If we assume that the absorption variability at low velocities originates close to the star, it is tempting to conclude that surface inhomogeneities modulate the DAC events when they are carried in the line of sight by the rotation. This could be in the form of a structured magnetic field or star spots caused by chemical anomalies, but a detailed investigation of these phenomena is not easily carried out. Such a model has some features in common with the CIR model of Mullan (1984). Since the estimated rotation period for ξ Per is less than 2.8 days (assuming $11R_{\odot}$ for the radius), several surface inhomogeneities or magnetic structures would simultaneously be needed to explain the short recurrence timescale ($\simeq$ 1 day). The phenomenon should be a rather permanent configuration, because long-term studies of ξ Per showed that the DAC pattern remains essentially unchanged (Kaper et al. 1990).

A different approach for explaining DACs has been recently put forward by Waldron et al. (1993). They consider DACs as caused by expanding density shells, which in their calculation mimic propagating "solitary waves". They compare their calculated doublet profiles and IR predictions with observations of ζ Pup, and find good agreement. Also in this model rotation is not incorporated, which will need further consideration.

Other evidence that stellar wind variations might be triggered from near the star's surface can be inferred from work on λ Cep O 6I(n)fp (Henrichs et al. 1990; Henrichs 1991). This star has shown a strong correlation between the near-photospheric He II 4686 emission line behavior and the stellar wind P Cygni line profile variations at extreme high velocities. In addition, the star λ Cep is a non-radial pulsator. The pulsations might provide the continuous driving mechanism for maintaining the wind

instabilities, but whether all O stars with DACs are non-radial pulsators is not clear. Fullerton (1990) concludes from his O-star survey that the line-profile variability in many O-stars could not be attributed to non-radial pulsations. An analysis of simultaneous optical and UV data is the only way to make progress. The results of such a campaign on ξ Per are described in a separate paper. An important partial result is summarized by Henrichs et al. (1993), who found that the DAC variability in ξ Per is related to the variability in Hα at low velocity, which also points to a near photospheric origin of DACs.

7. Conclusions

We have searched for stellar wind variability in 22 spectra of the O 7.5 giant ξ Per, taken within 3 days. Compared to earlier results, a much wider range in velocity space was found over which the wind is variable: from -100 to -2750 km s^{-1}. The latter is 400 km s^{-1} beyond the edge of the black bottom of saturated lines. These findings are supported by studying the time sequence of P Cygni profiles simultaneously in several ions. Correlated variability in the Si IV and N IV lines indicate that the variability, and therefore the DACs, are formed close to the stellar surface at rather low velocities. No significant variability in the emission part of the profiles was found. We argue that the high-velocity discrete absorption components, which appear in P Cygni lines of almost all O stars (and many B stars), are in fact the strongest manifestation of stellar wind variability, which includes the variability at low velocity (down to near zero) and at extreme high velocity in saturated P Cygni profiles. This is in qualitative agreement with a model in which a DAC is caused by expanding shock fronts arising from instabilities in the radiatively driven flow (Owocki et al. 1988; Owocki 1991; Puls et al. 1993). What triggers the appearance of DAC events remains unknown. Surface inhomogeneities at the base of the wind, carried into the line of sight by the rotation of the star, for instance in the form of magnetic structures, might play an important role. Further research in this direction is clearly needed.

Acknowledgements. HFH thanks Rolf Kudritzki and his colleagues for the pleasant and stimulating environment at the Universitäts Sternwarte and the Netherlands Organization for the Advancement of Pure Research (NWO) for a Christiaan and Constantijn Huygens fellowship, which made the first author's extended stay in München possible. Discussions with Stephan Haser, Stan Owocki, Joachim Puls and John Telting are highly appreciated. Special thanks go to Alex Fullerton for his detailed comments on the TVS method.

References

Barker, P.K., 1984, AJ, 89, 899
Bianchi, L., Bohlin, R.C., 1984, A&A, 134, 31
Castor, J.I., Abbott, D.C., Klein, R., 1975, ApJ, 195, 157
Conti, P.S., Ebbets, D., 1977, ApJ, 213, 438
Fullerton, A.W., 1990, Thesis, University of Toronto
Giddings, J., 1983a, IUE Newsletter, 12, 22
Giddings, J., 1983b, SERC Starlink User Note, 37
Gies, D.R., Bolton, C.T., 1986, ApJS, 61, 419
Groenewegen, M.A.T. and Lamers, H.J.G.L.M., 1989, A&AS, 79, 359
Harris, A.W., Sonneborn, G., 1987, in: Y. Kondo (ed.), *Scientific accomplishments of the IUE*, Reidel, Dordrecht, p. 729
Henrichs, H.F., 1984, Proc. 4th Europ. IUE Conf., ESA SP-218, p. 43
Henrichs, H.F., 1988, NASA/CNRS "O, Of and Wolf-Rayet Stars", Eds. Conti, Underhill, p. 199
Henrichs, H.F., 1991, ESO Workshop on Rapid variability of OB stars: Nature and diagnostic value, ed. D. Baade, p. 199
Henrichs, H.F., Kaper, L., Zwarthoed, G.A.A., 1988, Proc. Celebratory Symp.: A decade of UV astronomy with IUE, ESA SP-281, Volume 2, p. 145
Henrichs, H.F., Gies, D.R., Kaper, L., et al. 1990, Evolution in Astrophysics: IUE Astronomy in the era of new space missions, ESA SP-310, p. 401
Henrichs, H.F., Kaper, L., Ando, et al. 1993, Frontiers of Space and Ground-based Astronomy, eds. W. Wamsteker, M. S. Longair, and Y. Kondo, Astroph. Space Sc. Lib., Kluwer, Dordrecht, in press
Howarth, I.D. Prinja, R.K., 1989, ApJS, 69, 527
Kaper, L., Henrichs, H.F., Zwarthoed, G.A.A., Nichols-Bohlin, J.S., 1990, Proc. NATO Workshop on Mass Loss and Angular Momentum of Hot Stars, eds. L.A. Willson, G. Bowen, R. Stalio, p. 213
Kaper, L., Henrichs, H.F., Nichols-Bohlin, J.S., 1992, in: *Variable Stars and Galaxies*, (ed. B. Warner), ASP Conf. Series Vol. 30, p. 135
Kudritzki, R.-P., 1988, "Radiation in moving gaseous media", 18th Adv. Course Swiss Soc. of Astr. and Ap., Saas-Fee, p. 1
Lucy, L.B., 1983, ApJ, 274, 372
Mullan, D.J., 1984, ApJ, 283, 303
Owocki, S.P., Castor, J.I., Rybicki, G.B., 1988, ApJ, 335, 914
Owocki, S.P., 1991, NATO Workshop on Stellar Atmospheres: Beyond Classical Models, eds. I. Hubeny and L. Crivellari, Kluwer, Dordrecht, p. 235
Prinja, R.K., 1988, MNRAS, 231, 21P
Prinja, R.K. 1991, ESO Workshop on Rapid variability of OB stars: Nature and diagnostic value, ed. D. Baade, p. 211
Prinja, R.K., Howarth, I.D., 1986, ApJS, 61, 357
Prinja, R.K., Howarth, I.D., 1986, MNRAS, 233, 123
Prinja, R.K., Howarth, I.D., Henrichs, H.F., 1987, ApJ, 317, 389
Prinja, R.K., Barlow, M., Howarth, I.D., 1990, ApJ, 361, 607
Puls, J., Owocki, S.P., Fullerton, A.W., 1993, A&A, in press
Snow, T.P., 1977, ApJ, 217, 760
Snow, T.P., Jenkins, E.B., 1977, ApJS, 33, 269
St. Louis, N, Howarth, I.D., Willis, A.J., et al., 1993, A&A, 267, 447
Waldron, W.L., Klein, L., Altner, B., 1993, ApJ, preprint

This article was processed by the author using Springer-Verlag LaTeX A&A style file version 3.